*Key Engineering Materials*
*ISSN: 1662-9795, Vol. 926, pp 2162-2173*
*doi:10.4028/p-m5q583*

*Submitted: 2021-12-08*
*Revised: 2022-01-28*
*Accepted: 2022-01-28*
*Online: 2022-07-22*

# Identification of Anisotropic Yield Functions Using FEMU and an Information-Rich Tensile Specimen

Yi Zhang[1,a*], António Andrade-Campos[2,b], Sam Coppieters[1,c]

[1]Department of Materials Engineering, KU Leuven, Technology Campus Ghent, 9000 Gent, Belgium

[2]Department of Mechanical Engineering, Centre for Mechanical Technology and Automation, University of Aveiro, 3810-193 Aveiro, Portugal

[a]yi.zhang@kuleuven.be, [b]gilac@ua.pt, [c]sam.coppieters@kuleuven.be
*Corresponding author: Yi Zhang

**Keywords**: Anisotropic yield criteria; Material parameters identification; Heterogeneous mechanical tests; Inverse identification; DIC.

**Abstract**. To fully exploit the predictive accuracy of advanced anisotropic yield functions, a large number of classical mechanical tests is required for calibration purposes. The Finite Element Model Updating (FEMU) technique enables to simultaneously extract multiple anisotropic parameters when fed with heterogeneous strain fields obtained from a single information-rich experiment. This inverse approach has the potential to mitigate the experimental calibration effort by resorting to a single, yet more complex experiment augmented with Digital Image Correlation. In this paper, the sought anisotropic parameters of two selected yield functions are inversely identify for a low carbon steel sheet based on a previously designed information-rich tensile specimen. The experimentally acquired strain field data is used to inversely identify the Hill48 yield criterion and the Yld2000-2d yield functions. The results are compared with conventional calibration methods for both anisotropic yield functions. The inverse identification is then thoroughly studied using virtual experiments enabling to disentangle the effect of the material model error and the strain reconstruction error (DIC), respectively. It is shown that the material model error dominates the inverse identification of the Hill48 yield criterion. The reduced material model error for the Yld2000-2d yield function enables obtaining inversely identified anisotropic parameters that are closer to the reference ones. The paper clearly shows the importance of the predictive accuracy of the selected anisotropic yield function in the inverse identification process.

## 1 Introduction

Sheet metals typically exhibit an orthotropic plastic material behaviour related to the rolling process, causing different plastic behaviour along different directions [1]. The application of Finite Element Analysis (FEA) modelling to accurately simulate sheet metals forming behaviour heavily relies on the predictive accuracy of the adopted anisotropic yield function. Numerous anisotropic plastic constitutive models exist to precisely reproduce the anisotropic plastic material behaviour [2]. The more advanced models involve multiple anisotropic parameters requiring an extensive experimental campaign to accurately calibrate the model using conventional material tests. Strong proof of concept [1, 3-9] is available showing that a heterogeneous mechanical test along with an inverse identification strategy can reduce the experimental calibration effort. Assuming that the selected anisotropic yield function enables to describe the actual plastic material response, a well-designed heterogeneous mechanical test "activates" all anisotropic parameters leading to a robust and accurate inverse identification process. The strategy for such a strain heterogeneity design methodology has been proposed by Souto *et al.*[10]. It needs to be noted that the approach consists of accepting the shortcomings of the selected anisotropic yield function. In that case, a heterogeneous mechanical test should be designed in accordance with the forming process to be simulated afterwards [3]. This paper aims at a better understanding of the role of the selected anisotropic yield function in the inverse identification using FEMU [3]. The starting point of this paper is a previously designed tensile

specimen that maximizes the strain heterogeneity in the Area Of Interest (AOI) [10]. The material under investigation is a low carbon steel sheet that was fully characterized by Coppieters *et al*. [11] using conventional material tests yielding the reference values for the anisotropic parameters. The anisotropic parameters of both selected anisotropic yield criteria are inversely identified based on the heterogeneous experiment and compared with the reference. The assessment is based on the residual cost function values at reference and identified anisotropic parameters. The material model error is disentangled from the strain reconstruction error by resorting to virtual experimentation (FEDEF-module [12] in MatchID [13]) that enables to accurately mimic the complete DIC measurement chain. The paper is organized as follows. In Section 2, the selected anisotropic yield function and the reference parameters acquired from conventional material testing are introduced. In addition, the heterogeneous mechanical test is briefly discussed along with the FE model used in the FEMU process. Section 3 embarks on the experimental set up, the principles of FEMU and the metrics to quantify the identification quality. Section 4 presents the identification results and thoroughly investigates the role of the selected anisotropic yield function using virtual experimentation.

## 2 Numerical Procedure

### *2.1 Material model*

The test material used in this study is 1.2 mm thick industrial cold-rolled steel sheet. The plastic anisotropy of this material was characterized using an extensive experimental campaign reported by Coppieters *et al*. [11]. The isotropic elastic behavior was modelled using a Young's modulus *E* of 219 GPa and Poisson coefficient *v* of 0.3. The material is assumed to be plastically orthotropic, and two selected plane stress anisotropic yield functions are studied, namely the Hill48 yield criterion and the Yld2000-2d yield function. For the Hill48 criterion, the equivalent stress can be expressed as:

$$\sigma_{\mathrm{eq}}^{\mathrm{Hill48}} = F\sigma_{22}^2 + G\sigma_{11}^2 + H(\sigma_{11}-\sigma_{22})^2 + 2N\sigma_{12}^2, \tag{1}$$

with *F, G, H* and *N* being the anisotropic parameters. For Yld2000-2d [14], the equivalent stress can be calculated as:

$$\sigma_{\mathrm{eq}}^{\mathrm{Yld2000\text{-}2d}} = \left[\frac{1}{2}\left(\left|X_1^{'}-X_2^{'}\right|^M + \left|2X_2^{''}+X_1^{''}\right|^M + \left|2X_1^{''}+X_2^{''}\right|^M\right)\right]^{1/M}, \tag{2}$$

where the exponent "*M*" is a material parameter and typically based on the micro-structure and $X_i^{'}$, $X_i^{''}$ are the principal values of two stress tensors $\mathbf{X}^{'}$, $\mathbf{X}^{''}$. The model involves eight independent anisotropic parameters, $\alpha_i$ (with $i=1,...,8$). The selected anisotropic yield functions were integrated within the FEMU framework using the Unified Material Model Driver for Plasticity (UMMDp) [15]. Standard mechanical tests (uniaxial, biaxial tensile tests and multi-axial tube expansion tests) were used to calibrate the selected anisotropic yield functions and more details can be found in Coppieters *et al*. [11]. Table 1 shows the reference parameters obtained through the conventional test campaign. It must be noted that the evolution of the equivalent stress $\sigma_{\mathrm{eq}}$ as a function of the equivalent plastic strain $\varepsilon_{\mathrm{eq}}^{\mathrm{pl}}$ is considered to be known and determined from a uniaxial tensile test in the Rolling Direction (RD). The latter data is used to calibrate the strain hardening behavior using Swift's hardening law:

$$\sigma_{\mathrm{eq}} = K\left(\varepsilon_0 + \varepsilon_{\mathrm{eq}}^{\mathrm{pl}}\right)^n. \tag{3}$$

The identified model parameters, i.e. deformation resistance $K$, the initial strain $\varepsilon_0$ and the hardening exponent $n$ can be found in Table 1.

**Table 1** Calibrated Swift's hardening law parameters, Hill48 anisotropic model parameters at reference plastic strain $\varepsilon_0^{pl} = 0.1$ and Yld2000-2d parameters $\varepsilon_0^{pl} = 0.24$.

| Parameters-**Swift hardening** | $K$(MPa) | $\varepsilon_0$ | $n$ | Parameters-**Hill48** | $F$ | $H$ | $N$ |
|---|---|---|---|---|---|---|---|
| Reference-**RD** [1] | 594 | 0.0059 | 0.275 | Reference | 0.230 | 0.649 | 1.412 |

| Parameters-**Yld2000-2d** | $\alpha_1$ | $\alpha_2$ | $\alpha_3$ | $\alpha_4$ | $\alpha_5$ | $\alpha_6$ | $\alpha_7$ | $\alpha_8$ | $M$ |
|---|---|---|---|---|---|---|---|---|---|
| Reference | 0.9394 | 1.1841 | 0.8872 | 0.8765 | 0.9333 | 0.8020 | 1.0462 | 1.0227 | 5.90 |

[1] RD is used as a reference datum for work hardening.

*2.2 FEA model*

The heterogeneous specimen shape was designed using shape optimization driven by the maximization of the strain heterogeneity. More details can be found in [16]. It must be noted that slight geometrical deviations were observed between numerical specimen design and the manufactured specimen. Therefore, the final numerical geometry is a digitization of the manufactured specimen. Fig. 1(a) illustrates the geometry and Fig. 1(b) show local seed size, element formulation (S4R), boundary conditions and material orientation, respectively. Two material orientations are studied in this paper. In the first specimen, denoted as *Test C TD* (see Fig.1 (b)), the tensile direction was aligned with the Transverse Direction (TD). In the second specimen, denoted as *Test C R45,* the tensile direction is aligned with 45D (i.e. 45° with respect to the RD direction). As shown in Fig. 1, an AOI of 22 mm by 30 mm was used.

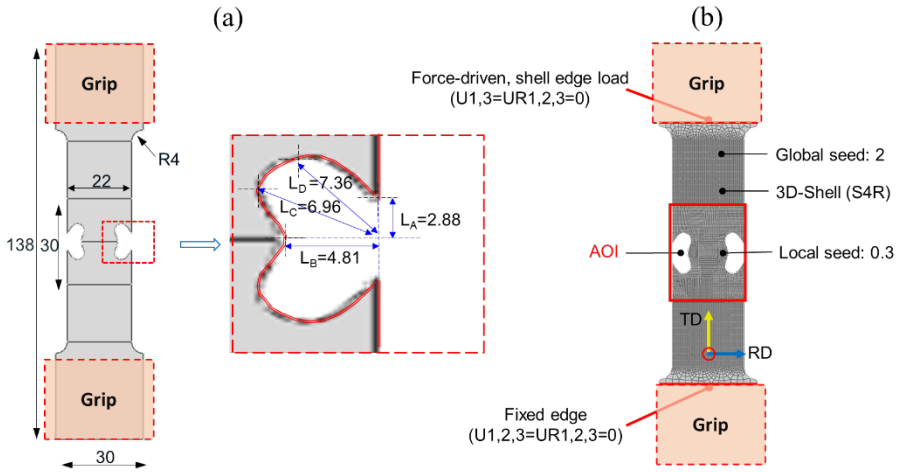


**Fig. 1** FE model information (a) specimen geometry, the units are in mm, (b) mesh information, element type, boundary conditions and material orientations for *Test C TD*.

## 3. Experimental Procedure

*3.1 Experimental Set-up*

The experiments (*Test C TD* and *Test C R45)* were conducted on a regular tensile machine with a load capacity of 10 kN using a constant crosshead speed of 5 mm/min ensuring quasi-static conditions. Stereo DIC was used to measure the displacement fields within the AOI using MatchID [13]. The DIC settings for the two tests are obtained by a DIC performance analysis as described in [17]. The detailed DIC settings for the two specimens are listed in Table 2. The stereo DIC system was synchronized with the load cell so that, for each image, the system records the corresponding tensile force. The experimental set up is illustrated in Fig. 2.

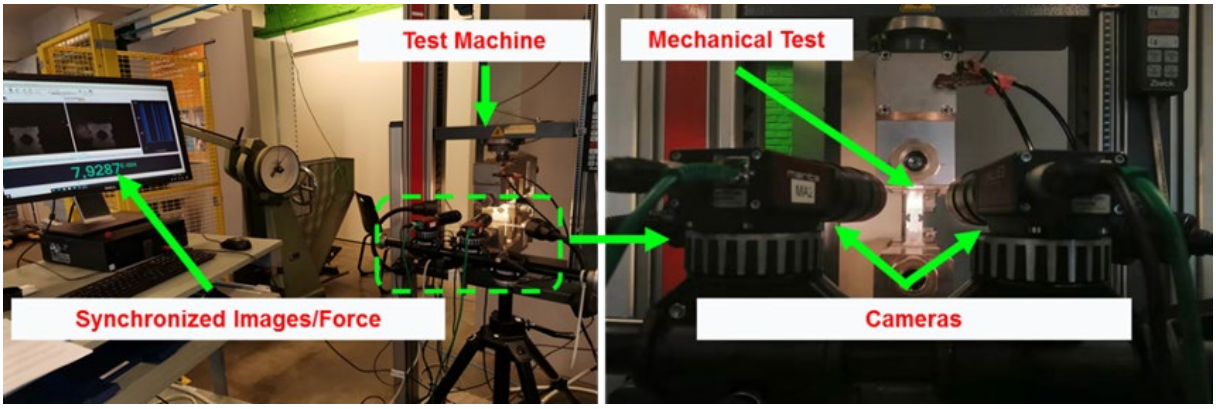


**Fig. 2** Uniaxial experimental test and DIC setup.

**Table 2** DIC settings after the performance analysis for *Test C TD* and *Test C R45*.

| **Specimens** | ***Test C TD*** | ***Test C R45*** |
|---|---|---|
| **Processing parameters** | **Specification/Value** | **Specification/Value** |
| Matching Criteria | ZNSSD | ZNSSD |
| Shape function | Affine | Affine |
| Interpolation function | Bicubic splines | Bicubic splines |
| Progress history | Spatial+update reference | Spatial+update reference |
| Subset size SS [px] | 21 | 31 |
| Step size(ST) [px] | 7 | 2 |
| Strain Window(SW) | 7 | 7 |
| Strain tensor-Polynomial | Euler-Almansi-Q4 | Euler-Almansi-Q4 |
| Virtual Stain Gauge(VSG) [px] | 63 | 43 |
| Pixel to mm conversion | 1 pixel= 0.0534 mm | 1 pixel= 0.0533 mm |
| Noise level [%] | 0.4140 | 0.4036 |

Fig. 3 shows the experimentally acquired tensile force as a function of the testing time. It can be inferred that both tests yield virtually the same global force response. Note that although force-time curves for the two-orientation tests are similar, they correspond to different deformation fields.

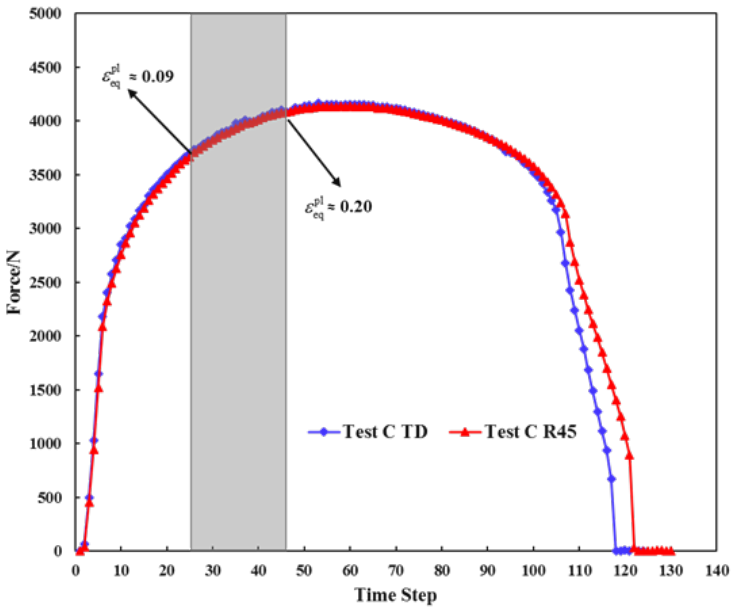


**Fig. 3** Force curves with respect to time step for *Test C TD* and Test *C R45*.

To investigate whether the identified parameters depend on the applied load level (e.g. second load step) and how much data (e.g. the number of load steps within the maximum of four load steps) is used in the identification, the following four different load level are considered (see Table 3) within the grey shaded box of Fig. 3.

**Table 3** DIC synchronized force were applied to the FE model at different load level for *Test C TD* and *Test C R45*.

| **Mechanical tests** | First Load step | Second Load step | Third Load step | Fourth Load step |
|---|---|---|---|---|
| ***Test C TD*** | 3.456 kN | 3.583 kN | 3.782 kN | 4.011 kN |
| ***Test C R45*** | 3.369 kN | 3.461 kN | 3.706 kN | 3.890 kN |

Each of the selected load steps corresponds to a similar maximum equivalent plastic strain within the AOI. As shown in Fig.3, the maximum equivalent plastic strain- $\varepsilon_{\mathrm{eq}}^{\mathrm{pl}}$ for the first load step and for the fourth load step is around 0.09 and 0.20, respectively. The most straightforward FEMU approach is to apply the measured tensile forces at the edges of the FE model, i.e. a force- driven simulation approach, as shown in Fig. 1(b). The experimental data associated with the four load steps are employed to inversely identify the plane stress Hill48 yield criterion as well as Yld2000-2d using FEMU.

3.2 *FEMU and identification quality assessment*

The basic principle of FEMU is to minimize the discrepancy between the experimental and numerical strain response by tuning the unknown anisotropic parameters of a chosen yield function used in the FE model. The Levenberg-Marquardt [18] algorithm is used to minimize $C(\boldsymbol{\theta})$. Given the force-driven simulation approach, only the strain discrepancy is considered by a least squares cost function that reads as:

$$\underset{\theta\in\mathbf{R}}{\text{minimize}} \quad C(\boldsymbol{\theta}) = \sum_{j=1}^{s}\sum_{i=1}^{n}\sum_{m}\left(\frac{\varepsilon_{\mathrm{m},ij}^{\mathrm{exp}} - \varepsilon_{\mathrm{m},ij}^{\mathrm{num}}(\boldsymbol{\theta})}{RMS_{\mathrm{m}}}\right)^2, \tag{4}$$

$$\text{with } RMS_m = \sqrt{\frac{1}{n}\sum_{i=1}^{n}\left(\varepsilon_{m,ij}^{\mathrm{exp}}\right)^2}, \qquad m = \mathrm{XX},\mathrm{YY},\mathrm{XY}, \tag{5}$$

where $\boldsymbol{\theta}$ is the vector of unknown anisotropic parameters and $n$ the number of data points in the DIC measurement at load step $j$. The $RMS_m$ (root mean square) value can be obtained by Eq. (5), which was used to normalize each strain component thereby eliminating the magnitude difference in Eq. (4). The subscripts "exp" and "num" indicate experimental and numerical response, respectively. The parameters identification quality can be expressed by the Average Relative Error (*A.R.E*) for all identified parameters as:

$$A.R.E = 100 * \frac{1}{k}\sum_{l=1}^{k}\left|\frac{\theta_l^{\mathrm{ref}} - \theta_l^{\mathrm{id}}}{\theta_l^{\mathrm{ref}}}\right|, \tag{6}$$

with $\boldsymbol{\theta}^{\mathrm{ref}}$ ($\boldsymbol{\theta} = \left[\theta_1, \theta_2, ..., \theta_k\right]^{\mathrm{T}}$, $k$ is the number of parameters for the selected anisotropic yield function) the vector of reference anisotropic parameters and $\boldsymbol{\theta}^{\mathrm{id}}$ the vector of inversely identified anisotropic parameters. Similarly, a second metric can be used to quantify the individual identification quality for $\theta_l$ via the individual relative error (*I.R.E*):

$$I.R.E = 100 * \left|\frac{\theta_l^{\mathrm{ref}} - \theta_l^{\mathrm{id}}}{\theta_l^{\mathrm{ref}}}\right|. \tag{7}$$

## 4. Result

### *4.1 Hill48 identification*

FEMU was fed with experimental data to identify the parameters of Hill48 model. The identified parameters of the Hill48 yield criterion obtained for *Test C TD* and *Test C R45* are reported in Table 4 and Table 5, respectively. The table shows the results for the identification using different individual load step experimental data (e.g., *Second load step* means only the second load step experimental data was fed in FEMU) as well as all load steps experimental data (*four load steps* means four load steps experimental data were fed in FEMU). Coppieters *et al*. [11] showed that the investigated material exhibits differential work hardening in the range $0 < \varepsilon_{eq}^{pl} < 0.03$. Isotropic hardening (i.e. the shape of the yield function is constant) is valid beyond this strain range. Given that the considered load steps generate strain levels that can be associated with isotropic hardening, it can be also inferred that the effect of considering single or multiple (4) load steps is marginal. From Table 4 and Table 5, it can be inferred that the identification of the parameter *H* is relatively stable and very accurately identified (<5%). Nevertheless, the overall identified parameter quality (*A.R.E*) is unacceptably high. The reason for this lies in the choice of the reference anisotropic parameters. Indeed, it was shown by Coppieters et al. [11] that the plastic behaviour of the test material cannot be accurately captured by the *r*-based (i.e., based on the Lankford coefficients) Hill48 yield criterion. This can be exemplified by computing the cost function when using the reference anisotropic parameters. For example, at second load step, this yields a cost function value of 30.65 which is considerably larger than the cost function after inverse identification, i.e. 9.89. This is basically a consequence of adopting an anisotropic yield function that cannot capture the actual material behaviour. The FEMU approach merely fits then the adopted model to the available experimental data by minimizing the discrepancy between the numerical and experimental strain field(s).

**Table 4** Comparison of reference parameters values and identified parameters values for *Test C TD* at different load step.

| ***Test C TD-*** Anisotropic parameters | ***F*** | ***H*** | ***N*** | ***A.R.E*** | **Cost function** | |
|---|---|---|---|---|---|---|
| **Reference values** | **0.2302** | **0.6492** | **1.4120** | | **30.65 (Real Exp)[1] 10.01 (Virtual Exp)[2]** | |
| **Initial guess** | **0.5** | **0.5** | **1.0** | | **Initial** | **Final** |
| First load Step $\varepsilon_{eq}^{pl}$=0.091 | 0.3221(40.06%) [1] | 0.6511 (0.33%) | 1.5334 (8.60%) | 16.33% | 20.16 | 10.46 |
| **Second load Step $\varepsilon_{eq}^{pl}$=0.109** | 0.3109 (31.19%) | 0.6595 (1.62%) | 1.6493(16.81%) | 21.99% | 19.78 | 9.89 |
| Third load Step $\varepsilon_{eq}^{pl}$=0.147 | 0.3001 (30.85%) | 0.6720 (3.54%) | 1.7226 (22.00%) | 16.20% | 20.96 | 9.68 |
| Fourth load Step $\varepsilon_{eq}^{pl}$=0.213 | 0.3525 (53.28%) | 0.6301(2.91%) | 1.5975(13.13%) | 23.11% | 26.74 | 13.30 |
| Four load Steps | 0.3053 (32.74%) | 0.6661(2.64%) | 1.6448(16.49%) | 17.29% | 45.54 | 20.31 |

[1] Cost function computed at reference parameters of Hill48 with real experimental data at second load step.
[2] Cost function computed at reference parameters of Hill48 with virtual experimental data at second load step.

The remaining discrepancy is the sum of several error sources [3, 8]:

- FEA discretization error: the FEA data needs to be interpolated to the DIC data points. This error mainly depends on the mesh size and here we conducted a mesh convergence study leading to a local element size of 0.3 mm.
- Geometry and the boundary conditions error, which is due to the approximation of the geometry and the boundary conditions in the FEA model. The geometry was derived from the manufactured sample, hence deemed sufficiently accurate. Given that the grips are far from the AOI, the force-driven approach is deemed to be accurate.
- Mapping errors between the FEA model and the experiment. Before the FEMU procedure, The coordinate systems was carefully aligned.

- Measurement errors (e.g. adopted DIC settings). The optimal DIC settings were obtained from performance analysis via MatchID module. Moreover, the influence of DIC measurement becomes negligible when large plastic deformation is of interest [8].
- Inaccurate anisotropic yield function.

Given the above, it can be concluded that the largest uncertainty is probably caused by the numerical material model. This was also a finding in the work of Cooreman et al. [3]. Nevertheless, it is until now unclear too which extent the DIC error plays a role of importance. To disentangle the role of a material model error and the DIC error, we resort to virtual (or synthetic) DIC experiments. Such synthetic data is generated based on an FE model that adopts a material constitutive model that is considered the ground truth. The displacements generated by this FE model are then used to numerically deform a speckle pattern. The data is then processed using a DIC code to retrieve the displacement fields and strain fields. The data can be used to compute the cost function. This approach enables to avoid the material model error and allows isolating the DIC error. For virtual experiment, it must be emphasized that, except for the method to obtain virtual experimental data, all other conditions (FE model, speckle pattern, image noise, DIC settings, etc.) and FEMU (initial guess, etc.) were kept identical with real experiment. It must be noted that the virtual experiment in this study was confined to 2D DIC, yet future work will embark on virtual stereo DIC experiments. The second load step was used to generate the virtual experiment using reference anisotropic parameters. For *Test C TD*, a cost function of 10.01 was found. Hence, the DIC error yields a contribution to the cost function of about 10.01. It needs to be noted that the DIC error (10.01) is larger than the final cost function (9.89) for second load step. This is normal because FEMU minimizes both the material model error and the DIC error. When looking at the cost function of *Test C TD* for the actual experiment using the reference anisotropic parameters, a value of 30.65 was found. As such, we can estimate the material model error by subtracting the theoretical DIC error (10.01) from the total cost function found in the experiment (30.65) yielding 20.64. The cost function when using isotropic values is 19.78, hence showing that there is a significant material model error explaining the observed gap between the inversely identified and the reference anisotropic parameters. All results for *Test C TD* are summarized in Table 4.

According to previous research [3-4, 8, 14], material orientation is of fundamental importance when it comes to identifying the plastic anisotropy of steel sheet. To investigate the material orientation influence for identified parameters, the same procedures were repeated for *Test C R45*.

The results are summarized in Table 5. It can be seen that the same order of magnitude is found for *A.R.E*, yet it appears to be more stable and independent of the considered load step. This could be interpreted as if the parameters obtained with the *Test C R45* are more repeatable than *Test C TD*. Additionally, the identified parameters of *N* is consistent (around 1.6), which can probably ascribed to the higher sensitivity of *N* in *Test C R45*. The virtual experiment is also conducted at second load step for *Test C R45*, and the DIC error is 42.19 as shown in Table 5. It is clear that the DIC error in this experiment is larger than *Test C TD.* This is probably related to the quality of the speckle pattern and DIC settings. For *Test C R45,* the cost function value at reference parameters for actual experimental data at second load step is 116.13, indicating that the $r$-based Hill48 criterion fails to reproduce the experiment. Indeed, the estimated model error is here 73.94 which is significantly larger than for *Test C TD* (20.55).

**Table 5** Comparison of reference parameters values and identified parameters values for *Test C R45* at different load step.

| ***Test C R45*- Anisotropic parameters** | ***F*** | ***H*** | ***N*** | | **Cost function** | |
|---|---|---|---|---|---|---|
| **Reference values** | **0.2302** | **0.6492** | **1.4120** | ***A.R.E*** | **116.13(Real Exp)[1] 42.19(Virtual Exp)[2]** | |
| **Initial guess** | **0.5** | **0.5** | **1.0** | | **Initial** | **Final** |
| First load Step $\varepsilon_{eq}^{pl}$=0.0916 | 0.3483(51.45%) | 0.6539(0.75%) | 1.5852(12.27%) | 16.33% | 64.78 | 43.84 |
| **Second load Step $\varepsilon_{eq}^{pl}$=0.1097** | 0.3524(53.24%) | 0.6514 (0.38%) | 1.5950(12.97%) | 22.19% | 59.67 | 35.36 |
| Third load Step $\varepsilon_{eq}^{pl}$=0.1487 | 0.3475(51.08%) | 0.6678 (2.89%) | 1.5971(13.11%) | 22.36% | 63.29 | 33.11 |
| Fourth load Step $\varepsilon_{eq}^{pl}$=0.2153 | 0.3272(42.27%) | 0.6833(5.28%) | 1.6268 (15.21%) | 20.92% | 69.01 | 33.11 |
| Four load Steps | 0.3439(49.50%) | 0.6549(0.91%) | 1.5999 (13.30%) | 21.24% | 125.00 | 70.23 |

[1] Cost function computed at reference parameters of Hill48 with real experimental data at second load step.
[2] Cost function computed at reference parameters of Hill48 with virtual experimental data at second load step.

Although it was previously shown a numerical study of Zhang *et al.* [16] that *Test C R45* exhibits a better identifiability than *Test C TD*, this could not be confirmed experimentally in this study due to the large material model error associated with the Hill48 yield criterion. Indeed, for a simple model such as the Hill48 model, it is clearly shown that the identified parameters largely depend on the adopted heterogeneous experiment. Similar conclusions were repeatedly reported [3, 8, 16], e.g. Coppieters *et al.* [20] argued that the validity of the inversely identified Hill48 yield function is confined to the experiment used in the FEMU procedure. The test configurations of *Test C TD* and *Test C R45* were designed to maximize the strain heterogeneity. This leads to an information-rich experiment which increases the probability of a good identifiability [16]. An important caveat, however, is that the plastic deformation in the test becomes more complex putting more demands on the accuracy of the selected material model (here the anisotropic yield function). Inverse identification of an "inferior" material model using a heterogeneous experiment, designed by maximizing the strain heterogeneity, is discouraged as it leads to a model calibration that is only valid for the considered heterogeneous experiment. In general, if the material models error is significant, Cooreman et al. [3] recommended to inversely identify parameters via designed mechanical test in accordance with the material forming which will be simulated afterwards. However, to the author's best knowledge, there has been no progress in designing a heterogeneous material test based on the dominating material states during a forming operation. The novelty in this section is that a unique method to disentangle the material model error from the DIC error in a heterogeneous experiment is proposed. Finally, our findings in this section suggest that more advanced constitutive models are required in conjunction with the adopted heterogeneous experiment. Hence, a more complex numerical model, namely, Yld2000-2d, was applied in the next section.

### *4.2 Yld2000-2d identification*

Exactly the same FEMU process with identical experimental data was employed to identify the parameters of the Yld2000-2d model for *Test C TD* and *Test C R45.* For a fair comparison with the reference parameters of Yld2000-2d model (calibrated at $\varepsilon_{eq}^{pl}$=0.24, as shown in Table 1), the experimental data from the fourth load step was used. Consequently, the anisotropic parameters of Yld2000-2d were identified at fourth load step for the *Test C TD* and *Test C R45*, respectively. Similar to Hill48, assuming $\sigma_{eq}$ as the yield stress in rolling direction [6], the following relation between the model parameters should be met:

$$\left|\frac{2\alpha_1+\alpha_2}{3}\right|^M+\left|\frac{2\alpha_3-2\alpha_4}{3}\right|^M+\left|\frac{4\alpha_5-\alpha_6}{3}\right|^M=2\,. \tag{8}$$

According to Eq. (8), one parameter becomes dependent to the others and therefore only seven of the $\alpha_k$ are identified by FEMU. The initial guess assumed isotropy, i.e. all the parameters were set to 1.0. The results are summarized in Table 6. Although the large amount of model parameters compared to the Hill48 model, the identification quality is much better for Yld2000-2D (*A.R.E,* 15.91%: *Test C TD,* 8.58%*: Test C R45)*.

**Table 6** Reference parameters, identified parameters and relative gap between these identified, and reference parameter sets for *Test C TD* and *Test C R45*.

| **Yld2000-2d** parameters | | **Initial guess** | ***Test C TD*** | ***Test C R45*** |
|---|---|---|---|---|
| 0 | **Ref** | 0 | **Identified** | **Identified** |
| $\alpha_1$ | 0.9394 | 1.0 | 0.8244 (12.24%) | 0.9793 (4.25%) |
| $\alpha_2$ | 1.1841 | 1.0 | 1.2119 (2.35%) | 1.1411 (3.64%) |
| $\alpha_3$ | 0.8872 | 1.0 | 1.3724 (54.69%) | 0.8422 (5.08%) |
| $\alpha_4$ | 0.8765 | 1.0 | 0.9092 (3.73%) | 0.8889 (1.42%) |
| $\alpha_5$ | 0.9333 | 1.0 | 0.9082 (2.69%) | 0.8496 (8.97%) |
| $\alpha_6$ | 0.8020 | 1.0 | 0.5203 (35.12%) | 0.5013 (37.49%) |
| $\alpha_7$ | 1.0462 | 1.0 | 1.0515 (0.51%) | 1.0238 (2.15%) |
| $\alpha_8$ | 1.0227 | 1.0 | 1.1860 (15.97%) | 1.0805 (5.65%) |
| *M* | 5.90 | 6.0-fixed | - | - |
| ***A.R.E*** | | | 15.91% | 8.58% |
| Cost function value at Reference parameter-**Hill48** [1] | | | 35.19 | 129.48 |
| Cost function value at Reference parameter-**Yld2000-2d** [2] | | | 31.87 | 58.71 |
| **DIC** error | | | 10.01 | 42.19 |
| Cost function value at identified parameter-**Yld2000-2d** | | | 10.59 | 30.14 |

[1] Cost function computed at reference parameters of Hill48 with real experimental data at fourth load step.
[2] Cost function computed at reference parameters of Yld2000-2d with real experimental data at fourth load step.

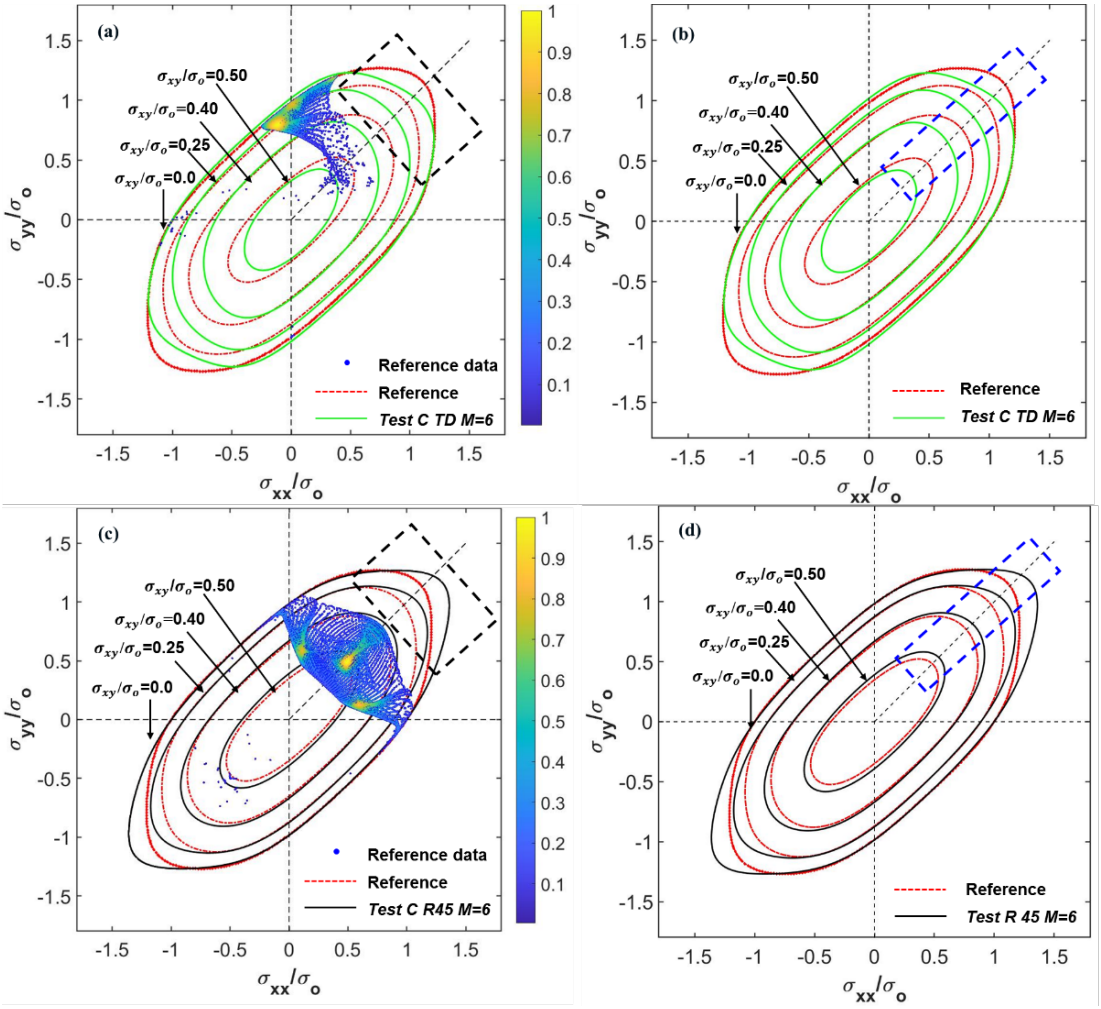


**Fig. 4** (a), (c) are comparisons of the reference Yld2000-2D yield loci (dashed red line) with identified yield locus (solid line), stress states distribution and corresponding density contour plot at reference parameters set for *Test C TD* and Test *C R45*, respectively; (b), (d) are used to purely compared reference yield loci with identified yield loci for *Test C TD* and *Test C R45* at different levels of $\sigma_{xy}/\sigma_0$, respectively.

Fig. 4 shows the comparison of the stress state distribution as well as its corresponding density contour plots using reference parameters (e.g., Fig.4 (a) and Fig.4 (c)). The reference yield loci and the inversely identified loci are shown Fig.4 (b) and Fig.4 (d) at different values of $\sigma_{xy}/\sigma_0$. It can be inferred that the inversely identified yield loci fit very well the stress states probed in *Test C TD* and *Test C R45*, as shown in Fig. 4. Due to the constraint expressed by Eq. (8), the two inversely identified yield loci coincide at uniaxial tension in the RD (aligned with x direction). Nevertheless, the inversely identified yield loci are inaccurate in regions (see dashed black rectangle in Fig. 4(a) and Fig. 4(c)) that do not contain experimental data. In that sense, Yld2000-2d seems to be merely fitted to the available experimental data. However, there are a number of observations that enable to arrive at a more advanced identification approach. First of all, it can be seen that with the increase of $\sigma_{xy}/\sigma_0$, the yield locus for *Test C TD* shows a larger discrepancy with the reference yield locus than the yield locus for *Test C R45,* which is illustrated by the dashed blue rectangles (see Fig. 4(b) and Fig. 4(d)). This indicates that a proper selection of the material orientation within the heterogeneous experiment can enhance the identifiability. As shown by Güner *et al*. [6], the experimentally measured equi-biaxial stress value can be included in the cost function to improve the identification quality. Yet, this solution increases the experimental work load again. The work of Zhang *et al*. [22] suggests that, based on an identifiability analysis, the identification error associated with $\alpha_7$ and $\alpha_8$ is caused by parameter interactions. An identification strategy that enables to mitigate the effect of parameter

interaction is currently investigated and will be published in a forthcoming paper. Finally, it must be noted that the problem can be solved if a complex tensile-load specimen is also used to add biaxial tension, as proposed by Macek et al.[23].

## 5. Conclusions

The FEMU technique combined with DIC is employed to inversely identify the Hill48 and Yld2000-2d function using a heterogeneous tensile specimen designed for maximum strain heterogeneity. From the analysis, two main conclusions can be drawn:

- A method based on virtual experimentation is proposed to disentangle the DIC error from the material model error. It is shown that for the material under investigation and the adopted heterogeneous experiment, the material model error associated with the Hill48 yield criterion is significantly larger than the error associated with the Yld2000-2d yield function.
- When using an optimized heterogeneous experiment that maximizes the strain heterogeneity, an accurate anisotropic yield function needs to be selected to enable proper identification. In case the material model error is significant, it is recommended to use a heterogeneous experiment that generates similar conditions as in forming process that will be simulated afterwards.

## CRediT authorship contribution statement standardization

**Yi Zhang**: Methodology, Software, Experiment, Formal analysis, Investigation, Writing - Original Draft. **Sam Coppieters**: Methodology, Experiment Investigation, Writing-Reviewing and Editing, Supervision, Formal analysis, Discussion. António Andrade-Campos: Reviewing and Discussion.

## Acknowledgements

Yi Zhang acknowledges the financial support from the program of China Scholarships Council (No.201806460097). Yi Zhang and Sam Coppieters acknowledge MatchID for the use of the MatchID software. Sam Coppieters and António Andrade-Campos gratefully acknowledge the support from the Research Fund for Coal and Steel under grant agreement No 888153.

## References

[1] Kim J H, Barlat F, Pierron F, et al. Determination of Anisotropic Plastic Constitutive Parameters Using the Virtual Fields Method. Experimental Mechanics [J], 2014, 54(7), pp.1189-1204.

[2] Banabic D, Carleer B, Comsa D S, et al. Sheet metal forming processes: Constitutive modelling and numerical simulation [M]. 2010.

[3] Cooreman S. Identification of the plastic material behavior through full-field displacement measurements and inverse methods, Free University of Brussels, Belgium, 2008, PhD thesis.

[4] Lecompte D, Cooreman S, Coppieters S, et al. Parameter identification for anisotropic plasticity model using digital image correlation: Comparison between uni-axial and bi-axial tensile testing. European Journal of Computational Mechanics [J], 2009, 18(3-4), pp.393-418.

[5] Zhang H, Coppieters S, Jimenez-Pena C, et al. Inverse identification of the post-necking work hardening behavior of thick HSS through full-field strain measurements during diffuse necking. Mechanics of Materials [J], 2019, 129, pp.361-374.

[6] Güner A, Soyarslan C , Brosius A , et al. Characterization of anisotropy of sheet metals employing inhomogeneous strain fields for Yld2000-2D yield function. International Journal of Solids and Structures [J], 2012, 49(25), pp.3517-3527.

[7] Prates P A, Oliveira M C, Fernandes J V. A new strategy for the simultaneous identification of constitutive laws parameters of metal sheets using a single test. Computational Materials Science [J], 2014, 85, pp.102-120.

[8] Wang, Yueqi, et al. Anisotropic yield surface identification of sheet metal through stereo finite element model updating. The Journal of Strain Analysis for Engineering Design [J], 2016, 51(8), pp.598-611.

[9] Lattanzi A, Barlat F, Pierron F, et al. Inverse identification strategies for the characterization of transformation-based anisotropic plasticity models with the non-linear VFM. International Journal of Mechanical Sciences [J], 2020, 173, pp.105422.

[10] Souto N, Thuillier S, Andrade-Campos A. Design of an indicator to characterize and classify mechanical tests for sheet metals. International Journal of Mechanical Sciences [J], 2015, 101-102, pp.252-271.

[11] Coppieters S, Hakoyama T, Eyckens P, et al. On the synergy between physical and virtual sheet metal testing: calibration of anisotropic yield functions using a microstructure-based plasticity model. International Journal of Material Forming [J], 2018, pp.741-759.

[12] Lava P, Cooreman S, Coppieters S, et al. Assessment of Measuring Errors in DIC Using Deformation Fields Generated by Plastic FEA. Optics and Lasers in Engineering [J], 2009, 47(7), pp.747-753.

[13] MatchID. 2021. Available online: https://www.matchid.eu/Software.html (accessed on 4 February 2021).

[14] Barlat F, Brem, J.C, Yoon, et al. Plane stress yield function for aluminum alloy sheets-part 1: theory. International Journal of Plasticity [J], 2003, 19(9), pp.1297-1319.

[15] Takizawa, H., Oide, K., Suzuki, K., et al. Development of the User Subroutine Library "Untied Material Model Driver for Plasticity (UMMDp)" for Various Anisotropic Yield Functions". Journal of Physics: Conference Series, 1063, July, p. 012099.

[16] Zhang, Y., Gothivarekar, S., Conde, et al. Enhancing the information-richness of sheet metal specimens for inverse identification of plastic anisotropy through strain fields. International Journal of Mechanical Sciences [J], 2021, p.106891.

[17] Gothivarekar, S., Coppieters, S., Van de Velde, et al. Advanced FE model validation of cold-forming process using DIC: Air bending of high strength steel. International Journal of Material Forming [J], 2020.13(3), pp.409-421.

[18] Levenberg, K., 1944. A method for the solution of certain non-linear problems in least squares. Quarterly of applied mathematics. 2(2), 164-168.

[19] Rossi, M., Pierron, F. and Štamborská, M., et al. Application of the virtual fields method to large strain anisotropic plasticity. International Journal of Solids and Structures [J], 97, 2016, pp.322-335.

[20] Coppieters S, Hakoyama T, Debruyne D, et al. Inverse yield locus identification of sheet metal using a complex cruciform in biaxial tension and digital image correlation. Inmultidisciplinary digital publishing institute proceedings, 2018 (Vol. 2, No. 8, p. 382).

[21] Martins, J.M.P., Andrade-Campos, et al. Calibration of anisotropic plasticity models using a biaxial test and the virtual fields method. International Journal of Solids and Structures [J], 2019. 172, pp.21-37.

[22] Zhang, Y., A. Van Bael, A. Andrade-Campos, et al. Parameter identifiability analysis: mitigating the non-uniqueness issue in the inverse identification of anisotropic yield criteria. International Journal of Solids and Structures [J], 2021, under review.

[23] Maček, A, Starman, B, Mole, N, et al. Calibration of Advanced Yield Criteria Using Uniaxial and Heterogeneous Tensile Test Data. Metals [J], 2020, 10, pp.542.